Journal of Oral Science, Vol. 56, No. 1, 17-22, 2014

Original

Effect of basic fibroblast growth factor on angiogenesis and bone regeneration in non-critical-size bone defects in rat calvaria

Risa Kigami[1)], Shuichi Sato[2,3)], Noriko Tsuchiya[1)], Nobuaki Sato[1)], Daigo Suzuki[1)], Yoshinori Arai[4)], Koichi Ito[4)], and Bunnai Ogiso[2,3,5)]

[1)]Division of Applied Oral Sciences, Nihon University Graduate School of Dentistry, Tokyo, Japan
[2)]Division of Advanced Dental Treatment, Dental Research Center, Nihon University School of Dentistry, Tokyo, Japan
[3)]Department of Periodontology, Nihon University School of Dentistry, Tokyo, Japan
[4)]Nihon University School of Dentistry, Tokyo, Japan
[5)]Department of Endodontics, Nihon University School of Dentistry, Tokyo, Japan

(Received October 7, 2013; Accepted December 25, 2013)

Abstract: We used microcomputed tomography (micro-CT) to evaluate the effects of basic fibroblast growth factor (FGF-2) contained in absorbable collagen sponges on angiogenesis and bone regeneration in rat calvarial non-critical-size bone defects. Two symmetrical non-critical-size calvarial bone defects (diameter, 2.7 mm) were created in male Fisher rats. An absorbable collagen sponge with or without FGF-2 (0.1% or 0.3%) was implanted into each defect. Blood vessel volume and bone volume were calculated using software. On day 28, blood vessel volume and bone volume were significantly greater in the 0.3% and 0.1% FGF-2 groups than in the control group. FGF-2 concentration-dependently increased blood vessels and bone formation in non-critical-size bone defects in rat calvaria. (J Oral Sci 56, 17-22, 2014)

Keywords: angiogenesis; bone; fibroblast growth factor; micro-computed tomography.

Correspondence to Dr. Shuichi Sato, Department of Periodontology, Nihon University School of Dentistry, 1-8-13 Kanda-Surugadai, Chiyoda-ku, Tokyo 101-8310, Japan
Fax: +81-3-3219-8349 E-mail: satou.shuuichi@nihon-u.ac.jp

doi.org/10.2334/josnusd.56.17
DN/JST.JSTAGE/josnusd/56.17

Introduction

Several growth factors are attracting interest because of their ability to actively regulate various cellular functions in angiogenesis and bone regeneration (1). Basic fibroblast growth factor (FGF-2) is a highly potent mitogen for cells of mesodermal origin and induces angiogenesis, which is essential for normal wound healing (2,3). In addition, *in vivo* studies have demonstrated that topical exogenous FGF-2 enhances healing of bone fractures (4,5). Bone is a highly vascularized tissue that remodels and repairs itself. New bone regeneration is facilitated by angiogenesis, ie, the formation of new microvessels from existing vessels (6,7). Angiogenesis and osteogenesis are important factors in orthopedic healing. Angiogenesis is an important process in bone formation and repair, and early vascular response is essential in fracture healing (8,9).

Critical-size bone defects are frequently studied in investigations of bone regeneration (10). We previously reported that angiogenesis enhances FGF-2 within rat calvarial critical-size bone defects; however, very little bone regeneration was observed (11,12). In the present study, we used microcomputed tomography (micro-CT) to investigate the effects of angiogenesis-driven bone reconstruction in the presence of FGF-2 in rat calvarial non-critical-size bone defects.

Materials and Methods

Animals

Forty male Fischer rats (weight 130-160 g) were housed in cages in an animal room (temperature, 22°C; humidity, 55%; 12/12-h light/dark cycle), with free access to food and water. The Animal Experimentation Committee of the Nihon University School of Dentistry, Tokyo, Japan approved this study (AP11D006).

Surgery for animals

Sodium pentobarbital (somnopentyl, 0.5 mL/kg body weight; Schering-Plough, Munich, Germany) was administered intramuscularly as general anesthesia, the skin of the surgical area was cleaned with 70% ethanol, and 0.5 mL lidocaine (xylocaine, 1:8 dilution; Astra Zeneca, Osaka, Japan) was injected intraperitoneally.

The dorsal cranium was incised along the sagittal suture. Two bone defects (width, 2.7 mm) were made in the dorsal parietal bones on both sides of the midsagittal suture. The midsagittal suture was not included in the bone defects, to eliminate any effects it might have on bone healing. We performed the surgery carefully, to avoid injuring the dura mater and sagittal sinus.

After washing out all bone fragments, an absorbable collagen sponge (ACS, Teruplug; Terumo Co., Tokyo, Japan) with or without FGF-2 was implanted into both bone defects (Fig. 1) and the skin was closed with silk sutures (Ethicon, Somerville, NJ, USA). The day of surgery is described as day 0.

Preparation of ACSs with and without FGF-2

FGF-2 (Kaken Pharmaceutical Co. Ltd. Tokyo, Japan) was frozen and dried. Each ACS was filled with 0.1% or 0.3% FGF-2. Control ACSs were prepared using 20 μL of aseptic saline solution.

Contrast perfusion by micro-CT

Ten rats were perfused with iopamidol radiographic contrast medium (Iopamiron; Bayer HealthCare AG, Leverkusen, Germany) on days 7, 14, 21, and 28. The front limbs were incised to the xiphoid process. One side of the sternum was cut using scissors, and the rib cage was retracted laterally. The descending aorta was clamped, and an angiocatheter was used to penetrate the left ventricle. The inferior vena cava was incised, and 20 mL heparinized saline (100 U/mL at 2 mL/min) was immediately perfused using a syringe pump. After perfusion with aseptic saline, the iopamidol solution was perfused to euthanize the animals. The perfusion was administered slowly, to reduce animal suffering.

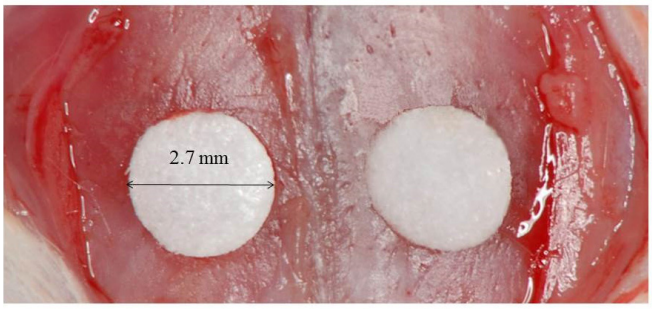

Fig. 1 ACS with and without FGF-2 in non-critical-size (diameter, 2.7 mm) calvarial bone defects.

Micro-CT analysis

Micro-CT (R_mCT; Rigaku, Tokyo, Japan) was used to assess bone regeneration and angiogenesis in specimens. Blood vessel formation was quantified based on perfusion of the vasculature with iopamidol. The exposure parameters were 90 kV and 88 μA. On day 0, we positioned a screen cylinder to overlap the initial bone defect. We then measured blood vessel volume (BVV) and bone volume (BV) within the cylinder on voxel images, using software (Kitasenjyu Radist Dental Clinic, i-View Image Center, Tokyo, Japan) that calculates gray values and corresponding numbers of voxels in regions of interest. A histogram of the X-ray absorption rate (*x*-axis) versus CT voxel number (*y*-axis) was constructed for the CT field of view. Histograms of the X-ray absorption rate showed peaks for hard and soft tissues, and the threshold was set at the value representing the trough between these peaks. The number of voxels that exceeded the threshold for the X-ray absorption rate was counted. Change in BVV was calculated by subtracting the value obtained from an image taken before angiography from that obtained from angiographic images of the bone defect each week. The space ratio filled with the BVV was measured for each bone defect (Fig. 2). BV was calculated as the number of bone-associated voxels multiplied by voxel volume. BVs in the regions of interest were measured weekly, under the same conditions, starting on day 0. BV gain was calculated by subtracting the day 0 value from each subsequent value. We evaluated the defect reossification ratio each week.

Tissue preparation and light microscopy

The experimental and control sites were evacuated, along with the surrounding bone and soft tissue, and fixed in 10% formalin on days 21 and 28. The specimens were then decalcified by soaking them in a formic acid-sodium citrate solution and embedded in paraffin. The sections

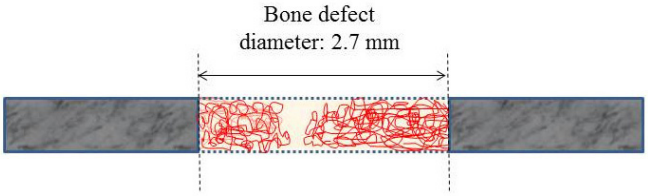

Fig. 2 Illustration of the area of interest. The extent of neoangiogenesis in defects was assessed by calculating change in blood vessel volume.

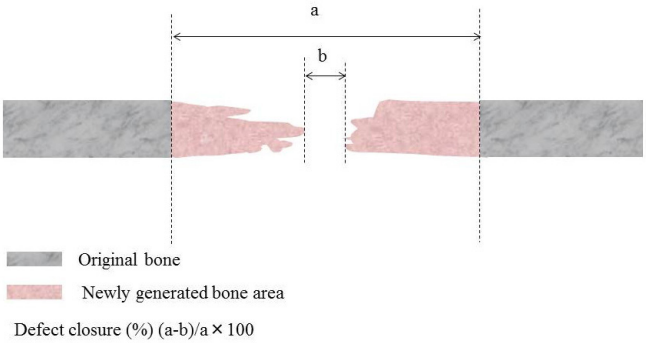

Fig. 3 Illustration of an osteotomy calvarial defect showing histometric analysis.

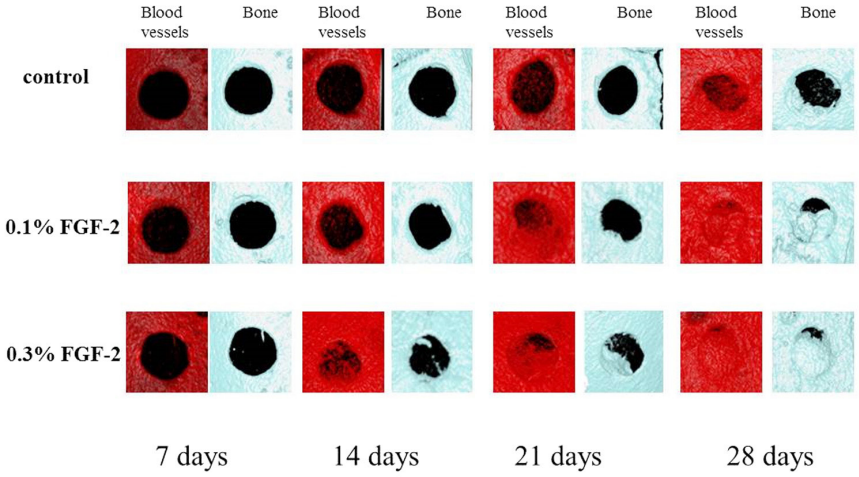

Fig. 4 Blood vessels: Angiographic images of calvarial bone defects at days 7-28 were processed using micro-CT imaging software.

were cut through the center of the bone defects and stained with hematoxylin and eosin. Histology sections were observed under a light microscope connected to a personal computer. Defect closure rate was defined as the distance between the margins of the defect and is presented as the percentage of total defect width. Newly generated bone (%) was defined as all tissues within the boundaries of the newly generated bone (Fig. 3).

The average numbers of osteoblast- and osteoclast-like cells in the new bone area were counted manually under light microscopy at 100× magnification.

Statistical analyses

The Kruskal-Wallis one-way analysis of variance by ranks test was used to assess reossification and BVV values obtained over time. A P value of <0.05 was considered to indicate statistical significance.

Results

Micro-CT analysis

New blood vessels began to appear around the edges of bone defects on day 7, and BVV increased until day 28 in all groups. BVV and BV were significantly greater in the 0.3% and 0.1% FGF-2 groups than in the control group, and in the 0.3% FGF-2 group versus the 0.1% FGF-2 group, on days 14, 21, and 28 (Figs. 4-6).

Light microscopy

Figures 7 and 8 show histological sections of cranial bone defects at 21 and 28 days after surgery. New bone had formed near the defect margins on day 21 in both FGF-2 groups (Fig. 7). In contrast, the control group showed no bone regeneration (Fig. 8).

More new blood vessels were observed in the FGF-2 groups than in the control group on days 21 and 28. On day 28, as compared with the 0.1% FGF-2 group, more new blood vessels and bone were observed in the 0.3% FGF-2 group, and new bone achieved better closure.

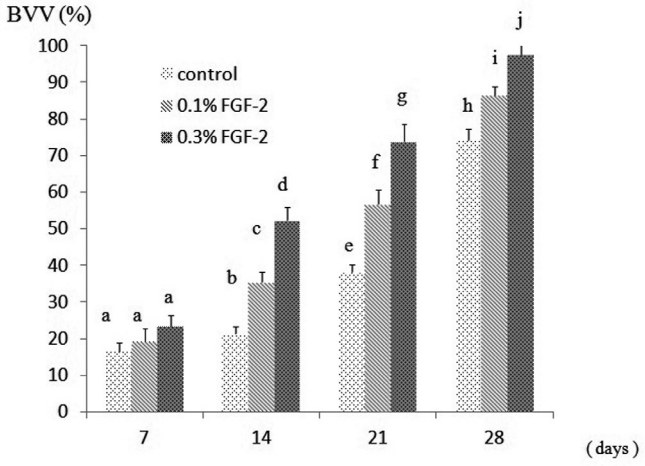

Fig. 5 Volume of new blood vessels. BVV was calculated as number of voxels multiplied by voxel volume. Values with the same letters indicate no significant statistical difference. Kruskal Wallis rank test, $P < 0.05$ ($n = 40$)

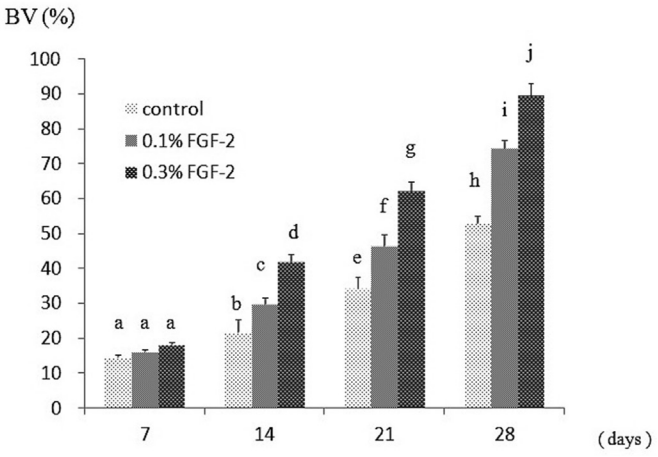

Fig. 6 Volume of newly generated bone. BV was calculated as number of voxels multiplied by voxel volume. Values with the same letters indicate no significant statistical difference. Kruskal Wallis rank test, $P < 0.05$, ($n = 40$)

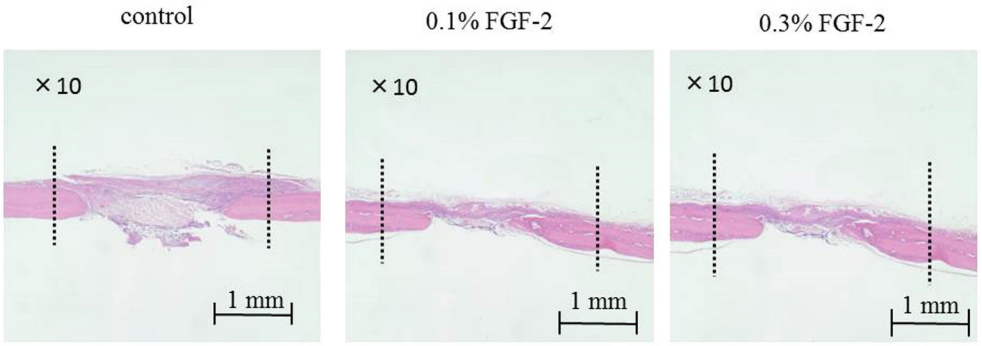

Fig. 7 Representative micrographs of tissue sections stained with hematoxylin and eosin on day 21. Dotted lines indicate edges of bone defects.

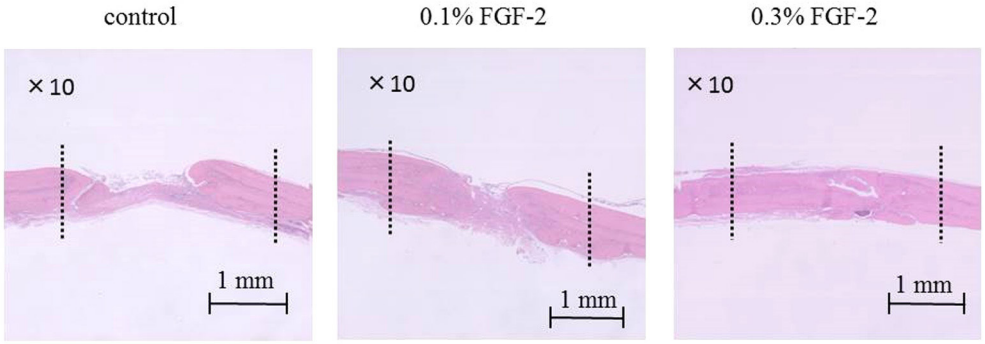

Fig. 8 Representative micrographs of tissue sections stained with hematoxylin and eosin on day 28. Dotted lines indicate edges of bone defects.

Bone regeneration induced by ACS with FGF-2 began at the edge rather than the center of the defect.

Histomorphometric analysis

There was significantly more new bone in the FGF-2 groups than in the control group (Table 1). In addition, as compared with control there were more new blood vessels and osteoblast- and osteoclast-like cells in the 0.1% and 0.3% FGF-2 groups on days 21 and 28. Numerous osteoclast-like cells were observed in the

Table 1 Amount of newly generated bone and defect closure

	21 days			28 days		
	Control	0.1% FGF-2	0.3% FGF-2	Control	0.1% FGF-2	0.3% FGF-2
New bone area	28.5 ± 0.4	43.9 ± 0.8*	56.9 ± 0.4*	43.6 ± 0.8*	75.8 ± 0.5*	85.2 ± 0.9*
Defect closure	39.2 ± 0.1	47.5 ± 0.5*	64.2 ± 0.2*	54.8 ± 0.6*	76.8 ± 0.7*	87.9 ± 0.8*

Unit, %, * Kruskal Wallis rank test, $P < 0.05$, $n = 10$

Table 2 Numbers of blood vessels and osteoblast- and osteoclast-like cells in newly generated tissue

	21 days			28 days		
	Control	0.1% FGF-2	0.3% FGF-2	Control	0.1% FGF-2	0.3% FGF-2
Blood vessel	11 ± 6	25 ± 8*	32 ± 16*	20 ± 8	33 ± 12*	47 ± 25*
Osteoblast-like cells	82 ± 31	117 ± 59*	152 ± 78*	163 ± 39	224 ± 36*	301 ± 75*
Osteoclast-like cells	2 ± 1	5 ± 2	7 ± 5*	6 ± 3	12 ± 5*	17 ± 5*

Unit, cells, * Kruskal Wallis rank test, $P < 0.05$, $n = 10$

0.3% FGF-2 group on day 28 (Table 2).

Discussion

We previously reported that angiogenesis enhanced FGF-2 within critical-size bone defects in rat calvaria; however, very little bone regeneration was observed (11). Therefore, in the present study we compared the effects of angiogenesis-driven bone repair in the presence of FGF-2 in rat non-critical-size bone defects.

Bone defects larger than a certain, or "critical," size cannot be repaired via bone augmentation (12). Non-critical-size bone defects close spontaneously and are repairable. Udagawa et al. (13) analyzed angiogenesis-driven bone repair in both critical-size and non-critical-size defects and suggested that capillary bed formation is important in understanding the difference in bone regeneration between critical-size and non-critical-size bone defects. The present study showed that new blood vessels began to appear around the edges of bone defects on day 7 after surgery in the FGF-2 groups. The capillary bed was formed on day 14 in the 0.3% FGF-2 group. On day 21, capillary bed formation was observed in both the 0.3% and 0.1% FGF-2 groups. The capillary bed connected one side of the defect to the other in the FGF-2 groups at a very early stage, on day 21. Blood vessel and capillary bed formation occurred earlier than in critical-size defects. Capillary bed connection accelerates blood flow, thus facilitating bone regeneration (6).

Bone regeneration began at the edge rather than the center of defects, probably because precursor cells of osteoblasts are necessary to initiate bone formation. Precursor cells in the periosteum differentiate into osteoblasts to induce bone formation (14). In this study, bone repair began from the periosteum, at the outer and inner surfaces near the defect, not from the surface of the bony edge around the original defect. Osteoblasts and their progenitors in the periosteum on both sides participated in forming projections of regenerated bone. FGF-2 induces angiogenesis in the periosteum.

We used a collagen carrier as scaffold, because collagen-based biomaterials are effective delivery vehicles for FGF-2. Collagen is also a good carrier for tissue regeneration. Murakami et al. (15) showed that FGF-2 delivered in a collagen or β-tricalcium phosphate collagen matrix stimulated healing in canine long bones.

We previously investigated the effects of other growth factors on animals in a GBA (guided bone augmentation) model (16,17). However, the characteristics of bone in those studies were inadequate for implant placement. Recently, the effect of local FGF-2 application on periodontal regeneration was investigated in a multicenter randomized clinical trial. The results indicated that FGF-2 was effective in periodontal tissue regeneration. Therefore, the use of FGF-2 may be an effective technique for bone regeneration in implant placement. A future study should examine the effects of FGF-2 in a GBA model.

In summary, FGF-2 induced angiogenesis and stimulated bone repair; its introduction into non-critical-size bone defects may be a suitable means of inducing rapid bone regeneration in conjunction with scaffolds that facilitate bone construction.

Acknowledgments

This work was supported in part by a Grant-in-Aid for Scientific Research C (No. 25463056) from the Japanese Society for the Promotion of Science.

References

1. Gerber HP, Ferrara N (2000) Angiogenesis and bone growth. Trends Cardiovasc Med 10, 223-228.
2. Bikfalvi A, Klein S, Pintucci G, Rifkin DB (1997) Biological roles of fibroblast growth factor-2. Endocr Rev 18, 26-45.
3. Kurokawa I, Hayami J, Kita Y (2003) A therapy-resistant chronic leg ulcer treated successfully with topical basic fibroblast growth factor. J Int Med Res 31, 149-151.
4. Mayahara H, Ito T, Nagai H, Miyajima H, Tsukuda R, Takemori S et al. (1993) In vivo stimulation of endosteal bone formation by basic fibroblast growth factor in rats. Growth Factors 9, 73-80.
5. Radomsky ML, Thompson AY, Spiro RC, Poser JW (1998) Potential role of fibroblast growth factor in enhancement of fracture hearing. Clin Orthop Relat Res 355, S283-293.
6. Carano RAD, Filvaroff EH (2003) Angiogenesis and bone repair. Drug Discov Today 8, 980-989.
7. Lambova SN, Müller-Ladner U (2010) Capillaroscopic pattern in systemic sclerosis--an association with dynamics of processes of angio- and vasculogenesis. Microvasc Res 80, 534-539.
8. Schmid J, Wallkamm B, Hämmerle CH, Gogolewski S, Lang NP (1997) The significance of angiogenesis in guided bone regeneration. A case report of a rabbit experiment. Clin Oral Implants Res 8, 244-248.
9. Glowacki J (1998) Angiogenesis in fracture repair. Clin Orthop Relat Res 355, S82-89.
10. Bosch C, Melsen B, Vargervik K (1998) Importance of the critical-size bone defect in testing bone-regenerating materials. J Craniofac Surg 9, 310-316.
11. Schmitz JP, Hollinger JO (1986) The critical size defect as an experimental model for craniomandibulofacial nonunions. Clin Orthop Relat Res 205, 299-308.
12. Kigami R, Sato S, Tsuchiya N, Yoshimakai T, Arai Y, Ito K (2013) FGF-2 angiogenesis in bone regeneration within critical-sized bone defects in rat calvaria. Implant Dent 22, 422-427.
13. Udagawa A, Sato S, Hasuike A, Kishida M, Arai Y, Ito K (2013) Micro-CT observation of angiogenesis in bone regeneration. Clin Oral Implants Res 24, 787-792.
14. Honma T, Itagaki T, Nakamura M, Kamakura S, Takahashi I, Echigo S et al. (2008) Bone formation in rat calvaria ceases within a limited period regardless of completion of defect repair. Oral Dis 14, 457-464.
15. Murakami S, Takayama S, Kitamura M, Shimabukura Y, Yanagi K, Ikezawa K et al. (2003) Recombinant human basic fibroblast growth factor (bFGF) stimulates periodontal regeneration in class II furcation defects created in beagle dogs. J Periodontal Res 38, 97-103.
16. Hasegawa Y, Sato S, Takayama T, Murai M, Suzuki N, Ito K (2008) Short-term effects of rhBMP-2-enhanced bone augmentation beyond the skeletal envelope within a titanium cap in rabbit calvarium. J Periodontol 79, 348-354.
17. Tsuchiya N, Sato S, Kigami R, Yoshimaki T, Arai Y, Ito K (2013) Effects of platelet-derived growth factor on enhanced bone augmentation beyond the skeletal envelope within a plastic cap in the rat calvarium. J Hard Tissue Biol 22, 221-226.